

On the discrimination of multiple phytoplankton groups from light absorption spectra of assemblages with mixed taxonomic composition and variable light conditions

EMANUELE ORGANELLI,^{1,2,*} CATERINA NUCCIO,¹ LUIGI LAZZARA,¹ JULIA UITZ,³ ANNICK BRICAUD,³ AND LUCA MASSI¹

¹Dipartimento di Biologia, Università degli Studi di Firenze, via Micheli 1, 50121 Florence, Italy

²Plymouth Marine Laboratory, Prospect Place, The Hoe, PL1 3DH Plymouth, UK

³Sorbonne Universités, UPMC Univ Paris 06, CNRS, UMR 7093, Laboratoire d'Océanographie de Villefranche (LOV), 181 Chemin du Lazaret, 06230 Villefranche-sur-mer, France

*Corresponding author: emo@pml.ac.uk

Received 17 January 2017; revised 30 March 2017; accepted 30 March 2017; posted 7 April 2017 (Doc. ID 284979); published 3 May 2017

According to recommendations of the international community of phytoplankton functional type algorithm developers, a set of experiments on marine algal cultures was conducted to (1) investigate uncertainties and limits in phytoplankton group discrimination from hyperspectral light absorption properties of assemblages with mixed taxonomic composition, and (2) evaluate the extent to which modifications of the absorption spectral features due to variable light conditions affect the optical discrimination of phytoplankton. Results showed that spectral absorption signatures of multiple species can be extracted from mixed assemblages, even at low relative contributions. Errors in retrieved pigment abundances are, however, influenced by the co-occurrence of species with similar spectral features. Plasticity of absorption spectra due to changes in light conditions weakly affects interspecific differences, with errors <21% for retrievals of pigment concentrations from mixed assemblages. © 2017 Optical Society of America

OCIS codes: (010.0010) Atmospheric and oceanic optics; (010.4450) Oceanic optics; (010.1030) Absorption; (010.0280) Remote sensing and sensors.

<https://doi.org/10.1364/AO.56.003952>

1. INTRODUCTION

Large differences in taxonomic and size structures of algal communities influence many ecological and biogeochemical marine processes. The various phytoplankton groups have different roles in the biogeochemical cycles of elements [1], and they are responsible for different contributions to total primary production [2]. Diatoms can contribute to 40% of total marine primary production [2,3] and together with dinoflagellates export carbon to deep waters. Coccolithophores, such as the bloom-forming species *Emiliania huxleyi* [4], sequester large quantities of calcium carbonate to form their characteristic external plates (coccoliths), thus reducing seawater alkalinity. Various phytoplankton types also release dimethyl sulphide (DMS) into the atmosphere [5–7], while others groups fix atmospheric nitrogen [8]. Hence, analysis of temporal and spatial variations of the phytoplankton community structure is of crucial importance to improve the understanding of biogeochemical fluxes in marine ecosystems, for instance, for modelling primary production and analyzing its climatic implications [7].

The synoptic detection and monitoring of changes in algal community structure can be pursued by the analysis of apparent and inherent optical properties derived from multispectral remote-sensing platforms [9–11]. Several bio-optical models were developed for the retrieval of products such as phytoplankton types, size classes, dominant size class, phytoplankton size distribution, or phytoplankton pigments [12,13]. In the perspective of the scheduled hyperspectral satellite missions (e.g., PACE and EnMAP missions), approaches based on *in situ* hyperspectral optical measurements were also successfully developed for the retrieval of pigment composition [14–16], size structure [17–20], or abundance of dominant species or groups [21–26].

Among the multispectral and hyperspectral approaches, the analysis of the spectral variations of the phytoplankton light absorption coefficients does not require any empirical relationship or assumption on the relationship between algal community composition and phytoplankton biomass [12,27]. The rationale is that the spectral characteristics of the phytoplankton light absorption coefficients are affected by pigment composition, concentration,

and packaging within the cell [17,28–30]. In particular, all algal pigments have defined absorption bands in the visible region of the electromagnetic spectrum [30–32], which influence the spectral shape of phytoplankton light absorption. Considering the fact that various phytoplankton groups are characterized by different pigment suites [33], the spectral signature of light absorption tends to have a similar shape within the same taxonomic group [29]. Despite these mechanistic considerations, there are sources of uncertainties affecting the performances of these spectral-response-based approaches which require investigation [12,27]. Some phytoplankton groups share similar pigments [33], which could yield similar optical signatures. Cell size influences the pigment packaging [28,30] and modifies the flattening of the light absorption spectra [17]. In addition, intracellular pigment concentration, packaging, and thus absorption signatures vary as a function of changes in growth factors such as light, temperature, and nutrient availability [34–42]. For example, high growth irradiances induce reduction of the cellular concentrations of chlorophyll *a*, as well as of other photosynthetic pigments, while the relative contribution of photoprotective pigments increases with respect to chlorophyll *a* [42]. As a consequence, cellular pigment packaging decreases while light absorption coefficients per unit of pigment increase [41] and spectra become sharper.

As recently highlighted by international committees of experts and algorithm developers [12,43,44], the extent to which the uncertainties introduced by the plasticity and/or similarity of spectral light absorption coefficients limit the optical detection of phytoplankton still needs to be addressed. In particular, among the various concerns raised by the dedicated international community, the following questions are of primary interest: (1) what is the effect of light-driven spectral modifications in the accuracy of phytoplankton retrieval from light absorption coefficients, and (2) how many phytoplankton groups can be discriminated from

the bulk spectral light absorption properties of marine algal communities characterized by mixed taxonomic composition.

Hence, the main objective of this study is to investigate these major questions in order to provide exploitable information and limits for development and application of methods and algorithms for the optical retrieval of phytoplankton community structure [12,43]. For this purpose, a set of laboratory experiments was carried out on marine algal cultures, representative of different taxonomic groups and covering a broad size range, grown in controlled conditions under various irradiance intensities. Considering the dataset of phytoplankton light absorption spectra and high performance liquid chromatography (HPLC) pigment concentrations provided by the experiments, we aimed at (1) assessing the influence of light growth conditions on the intra- and interspecific variability of the spectral shape of the phytoplankton light absorption coefficients and analyzing the effects on the optical classification; (2) extracting the absorption signature of a given species from the bulk light absorption properties of assemblages with mixed taxonomic composition and quantifying the species abundance; and (3) evaluating the errors in retrieving the abundance of a phytoplankton species within a mixed assemblage using reference light absorption spectra from populations adapted to different light regimes. No algorithm development and/or validation are here proposed.

2. MATERIALS AND METHODS

A. Algal Cultures and Experimental Setup

Laboratory experiments were conducted on cultures of seven marine algal species representative of different taxonomic groups. The selected algal species covered a broad size range (0.6–23 μm) and were characterized by different suites of auxiliary and taxonomically significant pigments (see Table 1 for

Table 1. Abbreviation, Names, Comments/Formulas for Phytoplankton Pigments and Pigment Sums: PS (Photosynthetic) and PP (Photoprotective) Pigments^a

Abbreviation	Pigment	Comment/Formula	Taxonomic Affiliation
Chl <i>a</i>	Chlorophyll <i>a</i> (plus allomers and epimers)	Phytoplankton biomass index, except for <i>Prochlorococcus</i> sp.	
Chl <i>b</i>	Chlorophyll <i>b</i>	PS in <i>Tetraselmis</i> sp.	<i>Tetraselmis</i> sp.
Chl <i>c</i> ₁ + <i>c</i> ₂	Chlorophyll <i>c</i> ₁ + Chlorophyll <i>c</i> ₂	PS in <i>P. tricornutum</i> , <i>A. carterae</i> , <i>E. huxleyi</i> , <i>Cryptomonas</i> sp.	
Chl <i>c</i> ₃	Chlorophyll <i>c</i> ₃	PS in <i>E. huxleyi</i>	
Dv Chl <i>a</i>	Divinyl-chlorophyll <i>a</i>	Biomass index for <i>Prochlorococcus</i> sp.	<i>Prochlorococcus</i> sp.
Dv Chl <i>b</i>	Divinyl-chlorophyll <i>b</i>	PS in <i>Prochlorococcus</i> sp.	
Allo	Alloxanthin	PP in <i>Cryptomonas</i> sp.	<i>Cryptomonas</i> sp.
19'-BF	19'-Butanoyloxyfucoxanthin	PS in <i>E. huxleyi</i>	
Diad	Diadinoxanthin	PP in <i>P. tricornutum</i> , <i>A. carterae</i> , <i>E. huxleyi</i>	
Diato	Diatoxanthin	PP in <i>P. tricornutum</i> , <i>A. carterae</i> , <i>E. huxleyi</i>	
Fuco	Fucoxanthin	PS in <i>P. tricornutum</i> , <i>E. huxleyi</i>	<i>P. tricornutum</i>
Lute	Lutein	PP in <i>Tetraselmis</i> sp.	
19'-HF	19'-Hexanoyloxyfucoxanthin	PS in <i>E. huxleyi</i>	<i>E. huxleyi</i>
Perid	Peridinin	PS in <i>A. carterae</i>	<i>A. carterae</i>
Viola	Violaxanthin	PP in <i>Tetraselmis</i> sp.	
Zea	Zeaxanthin	PP in <i>Synechococcus</i> sp., <i>Prochlorococcus</i> sp.	<i>Synechococcus</i> sp.
Pigment Sum		Formula	
TChl <i>a</i>	Total chlorophyll <i>a</i>	Chl <i>a</i> + Dv Chl <i>a</i>	
TP	Total pigments	Allo + 19' - BF + Fuco + 19' - HF + Perid + Zea + Chl <i>b</i> + Chl <i>a</i> + Dv Chl <i>b</i> + Dv Chl <i>a</i> + Chl <i>c</i> ₁ + <i>c</i> ₂ + Chl <i>c</i> ₃ + Diadino + Diato + Lute + Viola	

^aTaxonomic affiliation of marker pigments is indicated for examined species.

details and symbols; [45,46]). The prymnesiophyte *Emiliania huxleyi* [Roscoff Culture Collection (RCC) 904] and the two cyanobacteria *Synechococcus* sp. (RCC 322) and *Prochlorococcus* sp. (Med4, ecotype High Light 1; RCC 151) were obtained from the Roscoff Culture Collection (France). The diatom *Phaeodactylum tricorutum* was provided by the Stazione Zoologica Anton Dornh (Naples, Italy). The dinoflagellate *Amphidinium carterae* and the cryptophyte *Cryptomonas* sp. were isolated from Ligurian and Tyrrhenian waters (Mediterranean Sea) and identified at the University of Florence (Italy) according to Steidinger and Tangen [47] and Butcher [48], respectively. The prasinophyte *Tetraselmis* sp. was isolated from a live food pack used for aquaculture and then identified following the description reported by Thronsen [49].

Species were cultured in natural sterile seawater (Mediterranean Sea) with the addition of nutrients. The enriched seawater media were *f/2* medium [50,51] for *P. tricorutum*, *Cryptomonas* sp., and *Tetraselmis* sp.; *f/2-Si* medium (modified from [51]) for *A. carterae*; K medium [52] for *E. huxleyi*; and PCR-S11 medium [53] for *Synechococcus* sp. and *Prochlorococcus* sp.

Prior to each experiment, species were precultured for at least six generations in an exponential growth phase in order to ensure the acclimation to given irradiances. Population growth rates and division times were measured daily according to Wood *et al.* [54], using chlorophyll *a* *in vivo* fluorescence (Perkin-Elmer LS-5B; SLIT 5/5; excitation/emission 440/685 nm). Inoculated cultures of exponentially growing cells precultured at a given light intensity were gently stirred at regular intervals during the growth to avoid cell sedimentation, and to ensure a consistent level of light inside the vessel until sampling.

In a first experiment (hereafter “Experiment 1”), the seven species from different taxonomic classes were grown separately in batch cultures (300 mL) at $22 \pm 2^\circ\text{C}$ under three different irradiance conditions (10, 100, and $300 \mu\text{mol photons m}^{-2} \text{s}^{-1}$; 12/12 h light/dark (L/D) cycle) classified, respectively, as low light (LL), medium light (ML), and high light (HL). Different growth irradiances (10, 25, and $100 \mu\text{mol photons m}^{-2} \text{s}^{-1}$) for *Prochlorococcus* sp. were chosen as a result of insufficient growth rate ($<0.1 \text{ div/day}$) at $300 \mu\text{mol photons m}^{-2} \text{s}^{-1}$.

During a second experiment (hereafter “Experiment 2”), the species *P. tricorutum*, *A. carterae*, *E. huxleyi*, *Synechococcus* sp., and *Prochlorococcus* sp. were selected to simulate algal assemblages with mixed taxonomic composition. These species were chosen because of the broad size range they represented and because they are representative of major algal groups and phytoplankton functional types (i.e., silicifiers, calcifiers and DMS producers [1]) that can be encountered and coexist in various locations of the world’s open oceans [55–57]. In order to avoid interspecific competition for nutrients and light, the species were grown separately in batch cultures (3 L) at $22 \pm 2^\circ\text{C}$ under a photon flux density of $100 \mu\text{mol photons m}^{-2} \text{s}^{-1}$ (12/12 h L/D cycle). Then, just before sampling, the cultures were mixed to obtain 26 mixed assemblages (300 mL) with exact taxonomic structure. Desired taxonomic structures were achieved by varying the contribution to total chlorophyll *a* of each species, from 0% to 100% (increments of 20%), with the contribution of the other species decreasing at the same rate.

B. Bio-optical Analyses

Spectral light absorption coefficients (350–750 nm; resolution of 1 nm) were measured on filters using the transmittance–reflectance (T-R) method [58]. Culture samples (2–12 mL) of exponentially growing cells were filtered under low vacuum on glass-fiber filters (Whatman GF/F; Ø25 mm) and immediately stored at -80°C . Small volumes were sampled to avoid high optical densities (>0.3), outside the range where the correction for the path-length amplification factor (β) (see later) was established. Three replicates of each culture were analyzed using a LI-COR LI1800 spectroradiometer equipped with a LI-COR LI1800-12S integrating sphere, a LICOR LI1800-10 quartz fiber optic probe, and a halogen light source [59] (regularly calibrated and maintained). T-R measurements were carried out outside the sphere, before and after pigment extraction in methanol at 4°C for 24 h [60]. Optical densities were computed following Tassan and Ferrari [61]. Correction for the path-length amplification factor (β) was carried out according to Bricaud and Stramski [62]. New protocols have been recently proposed to decrease the uncertainty related to the β -factor correction [63,64] by using a specific instrument configuration that was not available at the time of measurements. However, the T-R method has been shown to address such an issue [64]. Therefore, it can be used as an alternative despite being a more laborious and time-consuming technique [64]. Optical densities were then converted into total [$a_p(\lambda)$] and nonpigmented particle [$a_{\text{NAP}}(\lambda)$] coefficients, and light absorption spectra of phytoplankton [$a_{\text{ph}}(\lambda)$] were finally determined by subtraction of $a_{\text{NAP}}(\lambda)$ from $a_p(\lambda)$.

HPLC analysis provided concentrations of 16 pigments including chlorophyll *a*, auxiliary chlorophylls, and carotenoids (Table 1). Up to three samples (2–25 mL) of each culture were filtered under low vacuum on glass-fiber Whatman GF/F filters (Ø25 mm) and immediately stored at -80°C . Pigment extraction was performed in 90% acetone at 4°C for 24 h. HPLC analysis was performed by a Class VP system (SHIMAZDU) equipped with a reverse-phase Shandon Hypersil MOS RP-C8 column, capable of resolving divinyl-chlorophyll *a* from chlorophyll *a*. The analysis was performed according to Vidussi *et al.* [65] and Barlow *et al.* [66] using the internal standard $\beta 8$ APO CAROTENAL (Fluka). Pigment concentrations were computed according to Mantoura and Repeta [67]. The sum chlorophyll *a* + divinyl-chlorophyll *a* concentration is referred to as TChl *a*, and total pigment (TP) is defined as the sum of all chlorophylls and carotenoids (Table 1).

Cell counts were performed using a light microscope Optiphot (Nikon) equipped with an Hg lamp for fluorescence. Culture samples (50 mL) were collected in dark glass flasks and immediately fixed with neutralized formalin to the final concentration of 1%. Cell numbers of micro- and nanoplanktonic species were counted using a Burkner hemacytometer with a $20\times$ objective, according to the manipulation, filling, and counting practices described in Guillard and Sieracki [68]. Cell numbers of *Synechococcus* sp. were counted by epifluorescence microscopy. Culture samples (25–150 μL) were filtered under low vacuum on Nuclepore black polycarbonate filters ($0.2 \mu\text{m}$, Ø25 mm). Details on sample preparation and counting ($100\times$ objective) are described in Guillard and Sieracki [68]. An average of three counts was used to estimate cell abundance for each batch

culture. Cell biovolume was calculated for each species (at least on 20 individuals) according to their geometrical shapes [69] and used to calculate the diameter of a sphere equivalent to cell volume. No count and biovolume calculation were performed for *Prochlorococcus* sp. Cell counting was performed only in Experiment 1 and used for calculation of cellular pigment content.

C. Statistical Analysis

The dataset produced with Experiment 1 was used to evaluate the intra- and interspecific spectral variability of the phytoplankton light absorption coefficients among the examined species as induced by different light growth conditions. First, the one-way analysis of variance (ANOVA) test (factor: light; levels: LL, ML, HL) was used to test the significance of intraspecific $a_{ph}(\lambda)$ variability at selected wavelengths. Since a small number of samples ($n = 3$) was analyzed within each level of the examined factor, F values of the ANOVA tests could be seriously affected by random variations; therefore, the nonparametric Kruskal–Wallis test [70] was used in parallel with the ANOVA. Levene's test (absolute deviations; $\alpha = 0.05$; [71]) of variance homogeneity was performed to test the assumptions of the ANOVA test. In very few cases the data variance failed to satisfy the homogeneity criterion; therefore the nonparametric Kruskal–Wallis test was used instead of the one-way ANOVA. Then the application of a hierarchical cluster analysis (HCA) to spectral absorption data (400–700 nm) was used to classify the light absorption spectra. The cluster trees (i.e., dendrograms) were obtained using the unweighted pair-group average linkage algorithm [72], which joined the clusters according to the average distance between all members. The cosine distance was chosen as criterion for evaluating the similarity level (from 0, i.e., no similarity, to 1, i.e., highest similarity) between each pair of objects following Torrecilla *et al.* [15]. The cophenetic correlation coefficient [73] was calculated to assess how faithfully the dendrogram preserved the pairwise distances between the examined samples. Cluster analysis was carried out by the free statistical software PAST version 3.04 [74].

The dataset produced with Experiment 2 was used to assess the feasibility to discriminate the contribution of a given species from bulk light absorption properties of assemblages with mixed taxonomic composition. For this purpose, the spectral similarity analysis introduced by Millie *et al.* [21] was used to extract the spectral signature of a species from a mixed assemblage. This method calculates the degree of similarity between two absorption spectra (i.e., similarity index, SI) by computing the cosine of the angle between two vectors such that [21]

$$SI = \frac{A_b \cdot A_c}{|A_b| \times |A_c|}, \quad (1)$$

where A_b is the absorption spectrum of a mixed assemblage and A_c is the absorption spectrum of a given species used as a reference. The cross operator (\cdot) is the vector product. The SI calculation, performed within the range 400–700 nm, yielded a number from 0 (i.e., no similarity between spectra) to 1 (i.e., highest similarity between spectra). Because the cosine distance was chosen as a criterion of similarity in both hierarchical cluster and spectral similarity analyses, the results and interpretation of

Experiment 1 can be extended to Experiment 2. Then, model I regression type was used to relate SI values to the relative abundance of a given species and the respective concentrations of marker pigments (MP) within mixed assemblages. A Student's *t*-test was performed to check the significance of the regression models. Then, the error in quantifying the MP concentrations from a range of representative SI values obtained from regression models was estimated using the percentage root mean square error (RMSE%) such that [75]

$$RMSE\% = 100 * \left(\sum_{i=1}^n \frac{(\bar{x}_i - x_i)^2}{n} \right)^{1/2}, \quad (2)$$

where \bar{x}_i and x_i were the estimated and measured MP concentrations, respectively.

Before applying both hierarchical cluster and spectral similarity analyses, each phytoplankton absorption spectrum (400–700 nm) was first smoothed using a simple moving average filter ($\Delta\lambda = 9$ nm [18]), then transformed by a normalized-ratio method (i.e., each data pair was divided by the largest of the pair [21]), and finally the corresponding fourth-derivative spectrum was computed by a finite approximation method assessing changes in curvature of a given spectrum over a sampling interval of 7 nm. The rationale of using the normalized-ratio transformation is twofold. First, it reduces the influence of broad peaks in the blue and red portions of the absorption spectra (due to chlorophyll *a*), which have similar traits in all algal species [21]. Second, it improves the sensitivity and linearity of the similarity index [21,24]. The fourth-derivative estimation enables a better separation of absorption bands and quantification of pigments [76].

3. RESULTS AND DISCUSSION

A. Intraspecific and Interspecific Variability of Light Absorption Spectra as Induced by Light Growth Conditions

In the following sections we present results and analysis for Experiment 1. Relationships between environmental factors (i.e., light, nutrients, and temperature) and bio-optical properties of various marine algal species and taxonomic groups have been reported and discussed by several studies both for natural (e.g., [36,77,78]) and controlled (e.g., [37–42]) conditions. Here we focus on the intracellular pigment contents and light absorption spectral characteristics of the seven marine algal species, useful to discuss the influence of different growth irradiances on their optical classification.

1. Influence of Light on the Intracellular Pigment Content

The algal pigment concentrations measured for the examined species varied with the three chosen light growth conditions (LL, ML, and HL; Table 2). According to previous studies [34,41,42], analysis of pigment modifications evidenced a common behavior among species, that is, the increase of the cellular total pigment and chlorophyll *a* contents as a consequence of the long-term acclimation to low irradiances. Recall also that all species were cultured under an excess of nutrients and, in synergy with limiting growth irradiances, this may cause an enhanced production of photosynthetic pigments

Table 2. Cellular Pigment Contents ($\mu\text{g cell}^{-1}$; fg cell^{-1}) for *Synechococcus* sp.) of Species Grown at 22°C Under Three Irradiances (E , $\mu\text{mol photons m}^{-2} \text{s}^{-1}$)^a

Species	E	Chl										TP	d				
		Chl c_3 (PS)	Chl $c_1 + c_2$ (PS)	Perid (PS)	19'-BF (PS)	Fuco (PS)	19'-HF (PS)	Viola (PP)	Diadino (PP)	Allo (PP)	Diato (PP)			Zea (PP)	Lute (PP)	Chl b^b (PS)	Chl a^b (PS)
<i>P. tricornutum</i>	10		0.06			0.30			0.03						0.58	0.97	6.24 ± 0.54
	100		0.05			0.25			0.06						0.27	0.64	6.50 ± 0.41
	300		0.03			0.15			0.07						0.16	0.42	[5.26 ± 1.13]
<i>A. carterae</i>	10		2.69	6.00				1.34							8.19	18.22	9.94 ± 0.80
	100		1.23	2.77				1.52							3.71	9.27	[12.5 ± 0.70]
	300		0.66	1.37				1.22							2.09	5.42	9.48 ± 0.65
<i>E. huxleyi</i>	10	0.10	0.08		0.007	0.005	0.41		0.02					0.41	1.05	3.44 ± 0.15	
	100	0.04	0.05		0.007	0.01	0.22		0.03					0.26	0.62	3.51 ± 0.11	
	300	0.04	0.05		0.004	0.02	0.22		0.09					0.26	0.71	[4.67 ± 1.20]	
<i>Cryptomonas</i> sp.	10		0.13							0.31				1.29	1.73	8.04 ± 0.40	
	100		0.05							0.25				0.77	1.07	7.99 ± 0.51	
	300		0.02							0.17				0.43	0.62	8.06 ± 0.37	
<i>Tetraselmis</i> sp.	10										0.32			4.81	8.92	8.16 ± 0.51	
	100										0.81			6.89	12.77	[9.44 ± 0.87]	
	300										0.27			2.86	5.65	8.39 ± 0.77	
<i>Synechococcus</i> sp.	10													1.97	2.59	[1.04 ± 0.11]	
	100													1.63	3.24	1.14 ± 0.14	
	300													1.30	2.63	1.14 ± 0.14	
<i>Prochlorococcus</i> sp.	10													0.71	1		
	25													0.56	1		
	100													0.46	1		

^aPigment contents for *Prochlorococcus* sp. are calculated as ratio (dimensionless) to the total pigment concentration (TP) because of cell count unavailability. See Table 1 for pigment abbreviations, comments, and formulas. The average diameter (d ; in μm) of a sphere equivalent to cell volume is reported together with the standard deviation for each species, except for *Prochlorococcus* sp.; brackets indicate growth conditions with significant changes in cell size (one-way ANOVA test, $p < 0.01$).

^bDv Chl b and Dv Chl a for *Prochlorococcus* sp., respectively.

[35,79]. TP cellular concentration of HL acclimated cultures was 0.68 (in *E. huxleyi*) to 0.26 (in *A. carterae*) times the cellular content observed in LL acclimated cultures (Table 2). Similarly, the Chl *a* per cell content of the HL acclimated cultures was 0.66 (*Synechococcus* sp.) to 0.26 (*A. carterae*) times that of LL acclimated cells (Table 2). The cellular contents of auxiliary chlorophylls and photosynthetic xanthophylls also decreased at the highest irradiances (Table 2). Differences among species were also observed. Chlorophylls $c_2 + c_1$ were the main auxiliary chlorophylls found in most studied species: a sharp reduction in cellular content with increasing irradiances was observed in *Cryptomonas* sp. and *A. carterae*; this was significantly smaller in *E. huxleyi* (Table 2). Considering photosynthetic xanthophylls, the cellular content of Peridinin in *A. carterae* varied from 1.37 pg cell⁻¹ in HL to 6.00 pg cell⁻¹ in LL conditions. The contents of Fucoxanthin in *P. tricornutum* and 19'-HF in *E. huxleyi* for LL conditions were twice those observed in HL conditions. In the case of photoprotective carotenoids, their cellular contents generally increased with increasing irradiances. For instance, Diadinoxanthin cellular concentration in *E. huxleyi* varied from 0.02 pg cell⁻¹ in LL to 0.09 pg cell⁻¹ in HL conditions, and Zeaxanthin in *Synechococcus* sp. increased from 0.62 to 1.61 fg cell⁻¹. Alloxanthin in *Cryptomonas* sp. was the only photoprotective pigment observed to decrease with increasing irradiances (Table 2), similarly to the results found by Schlüter *et al.* [80] for the cryptophyte *Plagioselmis prolonga*. Similar trends were also observed for pigment-to-TP ratios in the case of *Prochlorococcus* sp., for which no cell counts were available. Dv Chl *a* and Dv Chl *b* decreased with increasing irradiances, while the proportion of Zeaxanthin to TP increased from 23% in LL to 52% in HL conditions (Table 2).

2. Intraspecific Variability of Light Absorption Spectra

The phytoplankton light absorption spectra, normalized to their mean value between 400 and 700 nm ($a_{pb}^n(\lambda)$; [17]), of the seven species grown under three different light intensities are shown in Fig. 1. Each spectrum of a given light regime is the average of three replicates from the same culture, then normalized. Spectral coefficient of variation (CV%(λ), that is, the standard deviation to mean ratio) for each group of replicates was generally <15%. Spectral variability occasionally increased up to 27% between 550 and 700 nm. Values up to 35% and 40% were observed at a few wavelengths for *Prochlorococcus* sp. and *Synechococcus* sp., respectively, likely as a consequence of absent or less pronounced features of absorbing pigments other than Chl *a* or DV Chl *a*.

The three irradiance treatments caused changes in the spectral shape of phytoplankton light absorption coefficients. The first striking feature was a flattening of the absorption spectra associated with a change in the irradiance conditions from HL to LL. This was observed for all the studied species except *Cryptomonas* sp. [Fig. 1(d)]. This spectral flattening represented a stronger packaging of pigments within the cells [28,34]. In the case of the experimental conditions (fixed irradiance and excess of nutrients), the observed pigment packaging effect was mainly associated with the increase in the total intracellular pigment contents (Table 2) instead of changes in the average size [28]. Indeed, the one-way ANOVA test ($p < 0.01$) on the diameter of a sphere equivalent to cell volume revealed that the

small changes in cell size observed in the present dataset were significant only for some species or growth conditions (Table 2). A second observed feature is the variability in some spectral bands essentially associated to the absorption bands of carotenoids. The standard deviation spectrum highlighted the wavebands exhibiting maximum variability for each species, and the one-way ANOVA and Kruskal–Wallis tests confirmed, at these bands, significant effects of the irradiance treatments (Fig. 1; Table 3). This was especially striking for *Synechococcus* sp., for which the shape of the light absorption spectrum showed a drastic change (not just spectral flattening) from HL to LL conditions [Fig. 1(f)]. Considering the pigment-absorption band associations proposed by Bidigare *et al.* [31] and Hoepffner and Sathyendranath [32], these significant intraspecific differences in the spectral absorption signatures of the examined species were also related to modifications in intracellular concentrations of those pigments useful for taxonomic identification (Table 3).

In order to evaluate how changes in irradiance growth conditions influenced the classification of a given species through the entire absorption spectrum, we applied a HCA on the fourth derivative of the absorption spectra of the seven species used in Experiment 1. Recent studies [15,18,19,24,81] stressed the use of hyperspectral measurements and the potential of spectral derivative analysis for retrieving information on the phytoplankton community structure in the natural environment. Among the various methods used for pursuing this aim, the classification of algal assemblages using derivative spectra of light absorption through HCA worked successfully [15,19,81].

The dendrogram resulting from HCA yielded well-identified clusters, each comprising the three absorption spectra (LL, ML, and HL) from a single species (Fig. 2). The cophenetic correlation coefficient of 0.89 indicated highly reliable results of the cluster analysis. This suggests that even when different growth conditions provoke significant changes in cellular pigment concentrations and thus in the light absorption features as reported previously, the spectral absorption signature of a given phytoplankton species is still recognizable from that of other species. However, the similarity level at which the spectra of a species were identified as a cluster varied depending on the considered species. Somehow expected from unequally spaced growth irradiances, the distance between the spectra of the cultures acclimated to ML and HL conditions was shorter than that between the ML-acclimated and LL-acclimated spectra, except for *E. huxleyi* (Fig. 2). The similarity between LL-acclimated spectra and those for cultures acclimated to HL and ML conditions was, however, high for *P. tricornutum*, *A. carterae*, and *Cryptomonas* sp. (0.81–0.90). This suggested low intraspecific variability in the light absorption spectra for these species and examined growth conditions. The level of spectral similarity was instead lower than 0.68 for LL-acclimated spectra of *Tetraselmis* sp., *Synechococcus* sp., and *Prochlorococcus* sp. with respect to ML- and HL-acclimated cultures. This highlighted notable intraspecific differences, likely caused by the synergistic effect of limited light and excess of nutrients that enhanced pigment production [35,79] and provoked more drastic changes in the absorption spectral features.

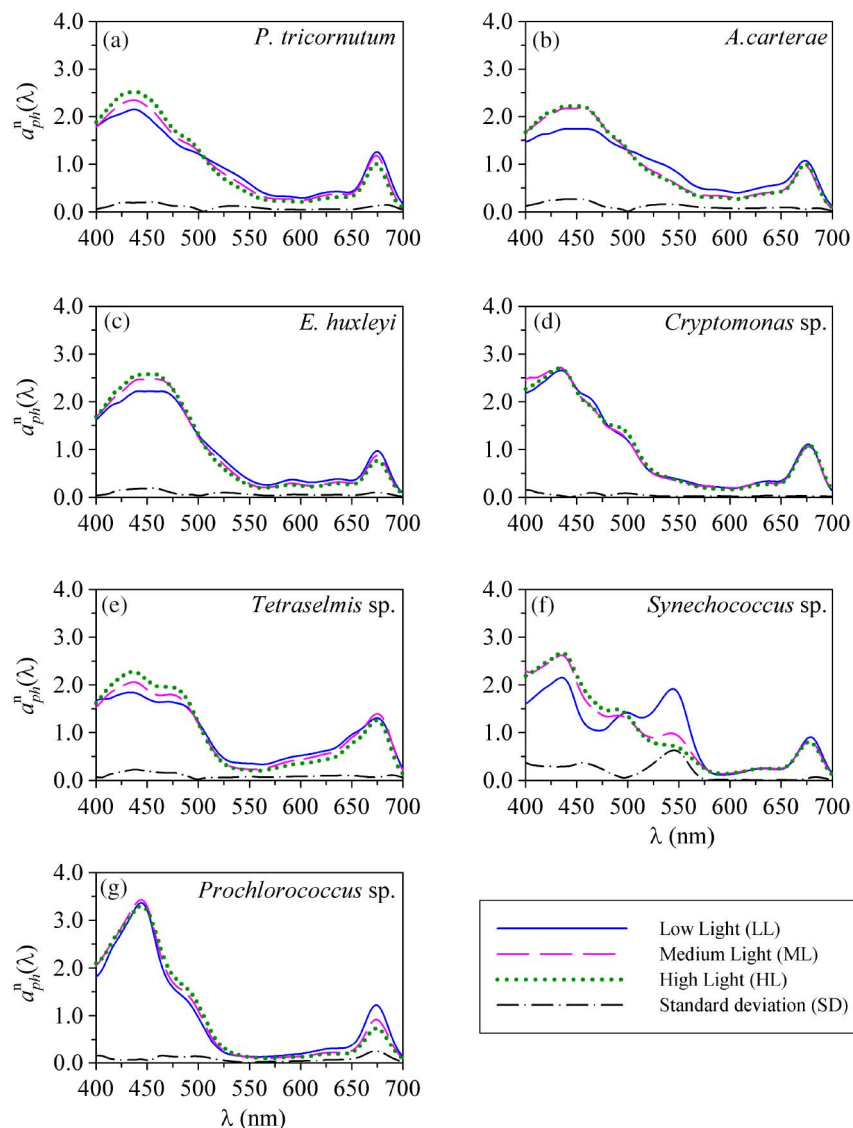


Fig. 1. *In vivo* light absorption spectra normalized to the mean between 400 and 700 nm [$a_{ph}^n(\lambda)$] for seven species grown at three irradiances. Each spectrum is the average of three replicates, then mean normalized. The standard deviation among the normalized spectra representing the three growth irradiances is also shown.

Table 3. Wavebands (λ ; nm) of Standard Deviation Maxima Calculated Between Mean-Normalized Absorption Spectra of Each Species Grown Under Three Light Regimes (Fig. 1)^a

Species	λ_1	λ_2	λ_3	λ_4	λ_5	λ_6
<i>P. tricornutum</i>	427 ^b	456 ^c	485 ^c	534 ^c (MP)	626 ^b	683 ^b
<i>A. carterae</i>	455 ^c	538 ^c (MP)	654 ^c	685 ^c		
<i>E. huxleyi</i>	456 ^c	492 ^b	523 ^c (MP)	594 ^c	675 ^c	
<i>Cryptomonas</i> sp.	465 ^c	498 ^c (MP)	640 ^c			
<i>Tetraselmis</i> sp.	438 ^c	470 ^b	643 ^c (MP)	689 ^c		
<i>Synechococcus</i> sp.	455 ^c (MP)	545 ^c				
<i>Prochlorococcus</i> sp.	465 ^c	496 ^b	676 ^c (MP)			

^aOne-way ANOVA and Kruskal-Wallis tests:

^bsignificant, $p < 0.05$;

^chighly significant, $p < 0.01$. MP, band associated to the corresponding marker pigment.

3. Interspecific Variability of Light Absorption Spectra

The next step of Experiment 1 was to quantify the differences between the shapes of the light absorption spectra among the

seven studied species (i.e., interspecific differences). For this purpose, a cluster analysis was applied to the fourth derivative of absorption spectra of each light growth condition (LL, ML,

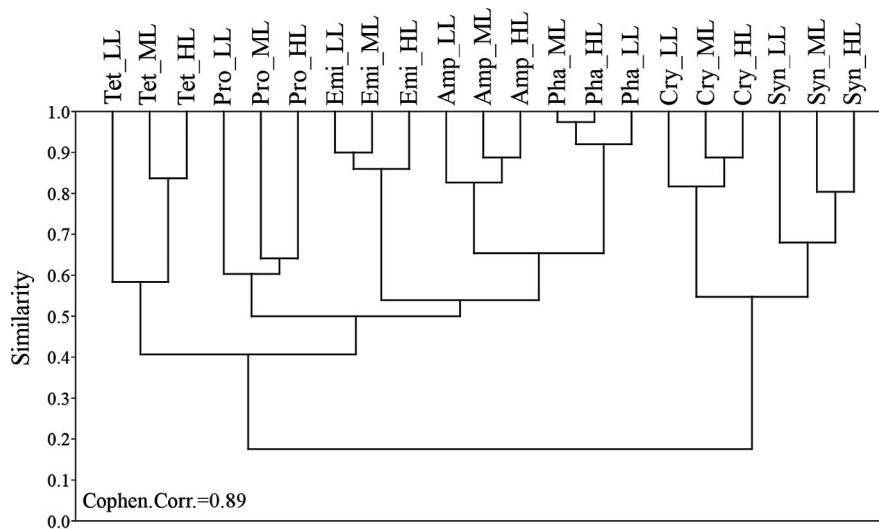


Fig. 2. Results of the HCA performed on the fourth-derivative of light absorption spectra (400–700 nm) of seven algal species for three different light growth conditions (LL, ML, and HL): *P. tricorutum* (Pha), *A. carterae* (Amp), *E. huxleyi* (Emi), *Cryptomonas* sp. (Cry), *Tetraselmis* sp. (Tet), *Synechococcus* sp. (Syn), *Prochlorococcus* sp. (Pro). The cophenetic correlation coefficient of the cluster analysis (Cophen. Corr.) is reported.

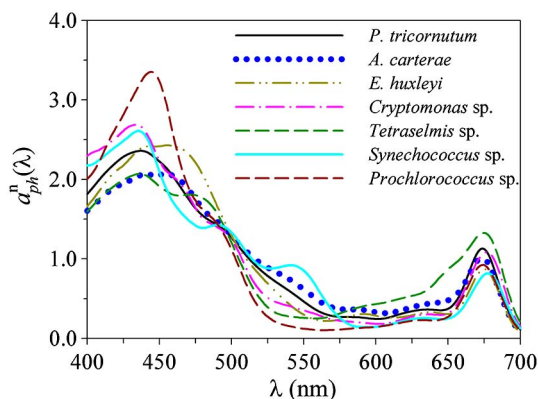


Fig. 3. *In vivo* light absorption spectra normalized to the mean between 400 and 700 nm [$a_{ph}^n(\lambda)$] computed as the average of the absorption spectra measured under LL, ML, and HL growth conditions (i.e., AS spectrum), then mean normalized.

and HL). In addition, we computed the average of the three absorption spectra obtained in the three different light conditions (Fig. 3) and applied a cluster analysis to the fourth derivative of the average spectra (hereafter AS).

The classifications of ML, HL, and AS spectra were similar with high cophenetic correlation coefficients (0.89–0.91). The results of this application evidenced that the absorption spectra of the examined species could be split into two major clusters [Figs. 4(b)–4(d)]. The first one was composed by the spectra of the cryptophyte *Cryptomonas* sp. and the cyanobacterium *Synechococcus* sp., which were characterized by a similarity ranging from 0.54 to 0.60. The second group included all the other species [Figs. 4(b)–4(d)]. Note that *Prochlorococcus* sp. is not displayed in Fig. 4(c) because of the insufficient growth rate observed at $300 \mu\text{mol photons m}^{-2} \text{s}^{-1}$. Within this cluster,

the absorption spectrum of the prasinophyte *Tetraselmis* sp. was the most different (similarity level between 0.39 and 0.55). The most similar spectra, indicating small interspecific differences as also recently observed by Xi *et al.* [81], were those of the diatom *P. tricorutum* and the dinoflagellate *A. carterae* (similarity level >0.69). The classification of absorption spectra obtained for the species grown in LL conditions (cophenetic correlation coefficient of 0.68) evidenced instead a high similarity between the spectra of the diatom *P. tricorutum* and the cryptophyte *Cryptomonas* sp. (similarity level of 0.63), and between the dinoflagellate *A. carterae* and the coccolithophore *E. huxleyi* within the other cluster [Fig. 4(a)].

The clusters given by this analysis could actually be explained by similarities and differences in pigment composition that characterized the examined species grown under fixed irradiance and nutrient-enriched conditions. *Cryptomonas* sp. and *Synechococcus* sp. were the only two species containing phycobilins such as phycoerythrin, a pigment with outstanding spectral signatures [82]. *P. tricorutum*, *A. carterae*, and *E. huxleyi* had the same accessory chlorophylls (chlorophyll *c*, Table 2) and photosynthetic xanthophylls (Fuco, Perid, and 19'-HF) with very similar spectral absorption signatures [30,31]. *Tetraselmis* sp. and *Prochlorococcus* sp. contained chlorophyll *b* and divinyl-chlorophyll *b*, respectively, two pigments with very similar light absorption features, and photoprotective pigments with optical properties close to those present in other cluster members. Another result of the cluster application to be emphasized is the low similarity observed between the two zeaxanthin-containing species *Prochlorococcus* sp. and *Synechococcus* sp. (Figs. 3 and 4). Given the similar cell size of these species (nominally 0.6 and 1 μm for *Prochlorococcus* sp. and *Synechococcus* sp., respectively), previous size-based absorption approaches detected these two species as a single group [17,18,83]. The low similarity here observed is probably related to the absorption bump at around 550 nm in *Synechococcus* sp.,

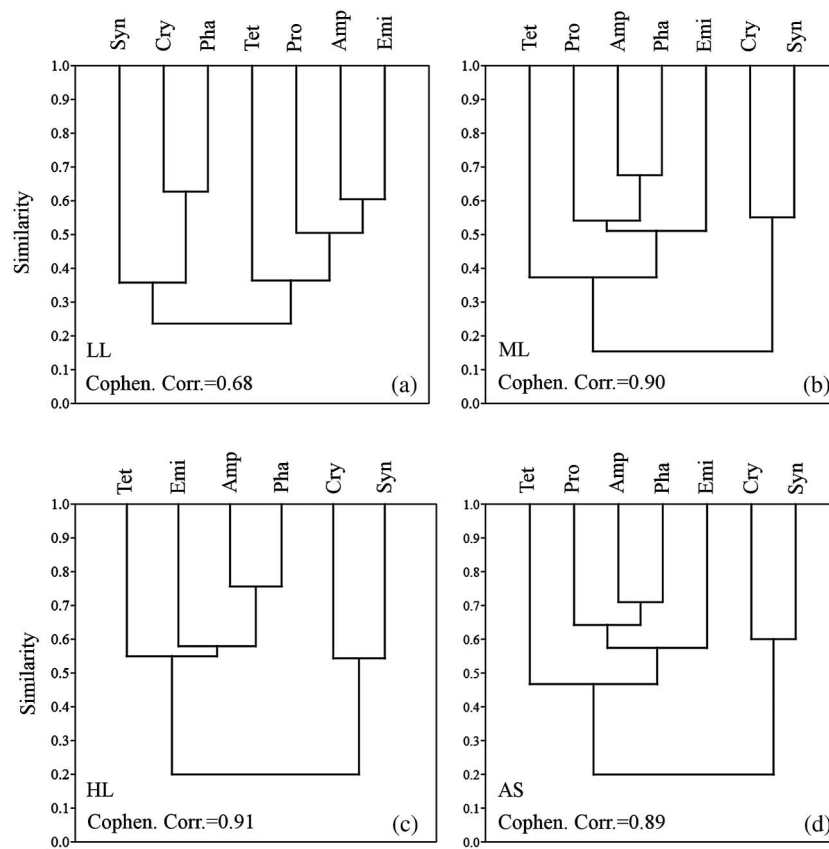


Fig. 4. Results of the HCA performed on the fourth derivative of light absorption spectra (400–700 nm) of seven algal species: (a) LL growth conditions ($10 \mu\text{mol photons m}^{-2} \text{s}^{-1}$); (b) ML growth conditions ($100 \mu\text{mol photons m}^{-2} \text{s}^{-1}$); (c) HL growth conditions ($300 \mu\text{mol photons m}^{-2} \text{s}^{-1}$); (d) absorption spectra representing the average of modifications induced by three different light growth conditions (AS spectra). In panel (c) *Prochlorococcus* sp. is not included because of the insufficient growth rate observed at $300 \mu\text{mol photons m}^{-2} \text{s}^{-1}$. In each panel, the cophenetic correlation coefficient of cluster analysis (Cophen. Corr.) is reported. Abbreviation of species name: *P. tricorutum* (Pha), *A. carterae* (Amp), *E. huxleyi* (Emi), *Cryptomonas* sp. (Cry), *Tetraselmis* sp. (Tet), *Synechococcus* sp. (Syn), *Prochlorococcus* sp. (Pro).

which may be due to the absorption of phycoerythrin, a pigment missing in *Prochlorococcus* sp. Although phycoerythrin abundance may have been drastically enhanced by the experimental high nutrient concentrations [79], this outcome suggests the possibility of using the pigment absorption signatures of these two species to distinguish their presence when they co-occur in the algal community.

B. Assessing the Contribution of a Given Species from Assemblages with Mixed Taxonomic Composition

In the following sections, the results obtained from Experiment 2 are presented. Discussion focuses on the feasibility to extract the absorption spectrum of a given species from the bulk absorption properties of an assemblage with mixed taxonomic composition and to quantify its contribution within it. Analysis is conducted with the spectral light absorption reference of a given species coming both from similar and different light growth conditions to that of mixed assemblages.

1. Taxonomic Structure and Bio-optical Characteristics of Simulated Algal Assemblages

Taxonomic structure and bio-optical characteristics of algal assemblages composed by varying proportions (in terms of TChl *a*)

of *P. tricorutum*, *A. carterae*, *E. huxleyi*, *Synechococcus* sp., and *Prochlorococcus* sp. (Experiment 2) are here presented and compared to those of natural assemblages in literature. It is acknowledged that the use of only one species to represent a taxonomic group cannot fully cover the intragroup variability and/or the intergroup similarities of light absorption spectral features that can be found in natural environments. The reduced taxonomical complexity of mixed algal assemblages helped minimize any change in cellular pigment content, cell number, and thus optical properties during the execution of the experiment. In addition, as a consequence of controlled and nutrient-enriched conditions of growth, simulated algal mixtures were characterized by total chlorophyll *a* concentrations higher than those of natural assemblages [30]. In terms of varying contributions of each species with respect to total chlorophyll *a*, taxonomic and bio-optical characteristics of simulated algal assemblages were however consistent with those observed in natural conditions.

The contribution of each phytoplankton size class in the simulated mixed algal assemblages, calculated according to Uitz *et al.* [83], ranged from contributions <13% up to more than 77%, a range of variation consistent with that of natural phytoplankton communities observed at the global scale [30]. The ratios of various groups of pigments (total chlorophylls *c*;

photosynthetic and photoprotective carotenoids) with respect to TChl a also varied with trends and within ranges similar (0–0.38, 0–0.90, and 0.16–1.29, respectively) to those observed in open ocean algal populations [30,57,84]. Only the ratios between photosynthetic carotenoids to total chlorophyll a increased with TChl a , while no specific trends were observed in natural populations [30,57,84]. Chlorophyll-specific phytoplankton light absorption coefficients at 438 and 675 nm [$a_{pb}^*(\lambda)$] of the simulated mixed assemblages varied in the ranges 0.025–0.20 and 0.011–0.057 $\text{m}^2 \text{mg TChl } a^{-1}$, respectively, and decreased as a function of TChl a according to a power law [$r^2 = 0.75$ for $a_{pb}^*(438)$ and $r^2 = 0.57$ for $a_{pb}^*(675)$]; [84]]. The observed coefficients were consistent with those observed for various open ocean waters [30,57,84–86], except the ultra-oligotrophic surface waters of the South Pacific Ocean [87]. However, $a_{pb}^*(675)$ values up to 0.057 $\text{m}^2 \text{mg TChl } a^{-1}$ instead of 0.038 $\text{m}^2 \text{mg TChl } a^{-1}$ [84,86] were observed in simulated mixed assemblages, which suggested a weaker pigment packaging effect of TChl a within algal cells than that found in natural assemblages.

The light absorption spectra of simulated mixed assemblages that will be used, in the following sections, to assess the capability of discrimination of a given species from bulk light absorption spectral properties are shown in Fig. 5. Each spectrum is the average of three replicates from the same mixed culture, then mean-normalized. Analysis of coefficients of variation [CV%(λ)] between replicates (calculated as the ratio of the standard deviation to the average spectrum) showed spectral variability varying between 1% and 20%, except on a few occasions. Instead, when observing CV%(λ) values resulting from a variety of mixed assemblages, regions of maximum spectral variability, that is, the wavebands of *in vivo* absorption of auxiliary pigments (marker pigments included; [30–32]) were evidenced (Fig. 5). High CV% values (up to 55%) were generally observed around 550 nm (Fig. 5), a source of variability that could be mainly ascribed to the varying proportions of phycoerythrin in *Synechococcus* sp., Fucoxanthin in *P. tricornutum*, Peridinin in *A. carterae*, and 19'-HF in *E. huxleyi*. High variability (up to 27%) was also observed at 590 and 640 nm, as a result of the variable occurrence of chlorophylls c , and within the range 400–500 nm (up to 16%), probably as a consequence of the different spectral contributions of the various photoprotective pigments.

2. Discrimination of a Given Species from Assemblages Adapted to the Same Light Regime

Previous studies have demonstrated the potential of the spectral similarity analysis [21] and use of SI (Eq. 1) for detecting and quantifying a given phytoplankton species from light absorption spectra, even in natural mixed assemblages [22]. SI values, as derived from pairwise comparison between a reference spectrum of a given species and that of an assemblage with unknown taxonomic structure, were observed to vary accordingly with the fraction of a species [21–23,25] or cell abundance [24]. SI was thus promoted as a possible quantitative indicator of the presence of given phytoplankton groups within assemblages [24]. Hence, in order to investigate the possibility to detect the spectral signature of multiple species and quantify their abundances within mixed assemblages, we applied here the spectral similarity analysis on the fourth derivative of absorption spectra of the algal assemblages

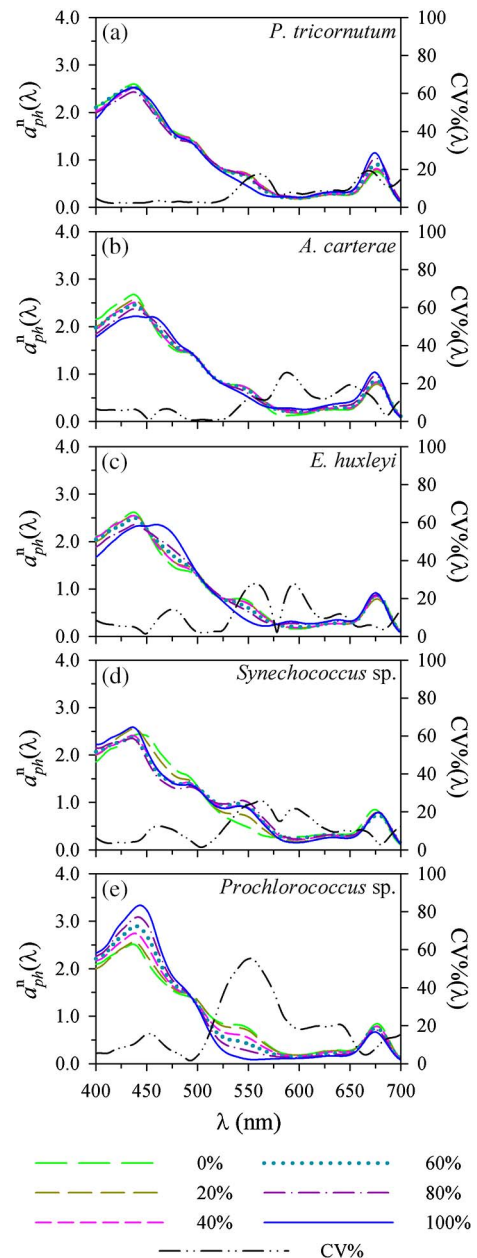


Fig. 5. *In vivo* light absorption spectra normalized to the mean between 400 and 700 nm [$a_{pb}^n(\lambda)$] of 26 mixed assemblages obtained using five cultured species together with the spectral coefficient of variations [CV%(λ)]. Each spectrum is the average of three replicates, then mean-normalized. Assemblages were obtained varying the contribution to TChl a of a species at a time from 0 to 100% (20% steps): (a) *P. tricornutum*, (b) *A. carterae*, (c) *E. huxleyi*, (d) *Synechococcus* sp., (e) *Prochlorococcus* sp.

simulated during Experiment 2. In this context, and differently from other algorithms (e.g., [18]), spectral similarity analysis can be applied regardless of any prior model training.

The index of spectral similarity, SI, was first computed between the spectra measured for each simulated mixed assemblage where the contribution of a given species varied from 0% to 20% of TChl a , and the reference spectrum of the corresponding species. The absorption spectrum of a given species

cultured at a light intensity of $100 \mu\text{mol photons m}^{-2} \text{s}^{-1}$ and obtained from Experiment 1 was chosen as the reference spectrum, as it represented the same experimental light conditions as those of the mixed assemblages. Hence, this comparison allowed investigating the discrimination among species regardless the influence of light-induced spectral modifications. The resulting SI was then regressed against (1) the relative abundance (in term of TChl *a*) of the considered species within the mixed assemblage

and (2) the log₁₀ concentration of the corresponding marker pigment (Fig. 6). Marker pigments were chosen as indicative of the abundance of a given species within the assemblage following Jeffrey and Vesk [45].

The resulting SI values were related to the fraction of a given species within the assemblages ($r^2 > 0.68$, Table 4, Fig. 6 left column) and to the concentration of the corresponding marker pigment ($r^2 > 0.83$, Table 4, Fig. 6 right column). These

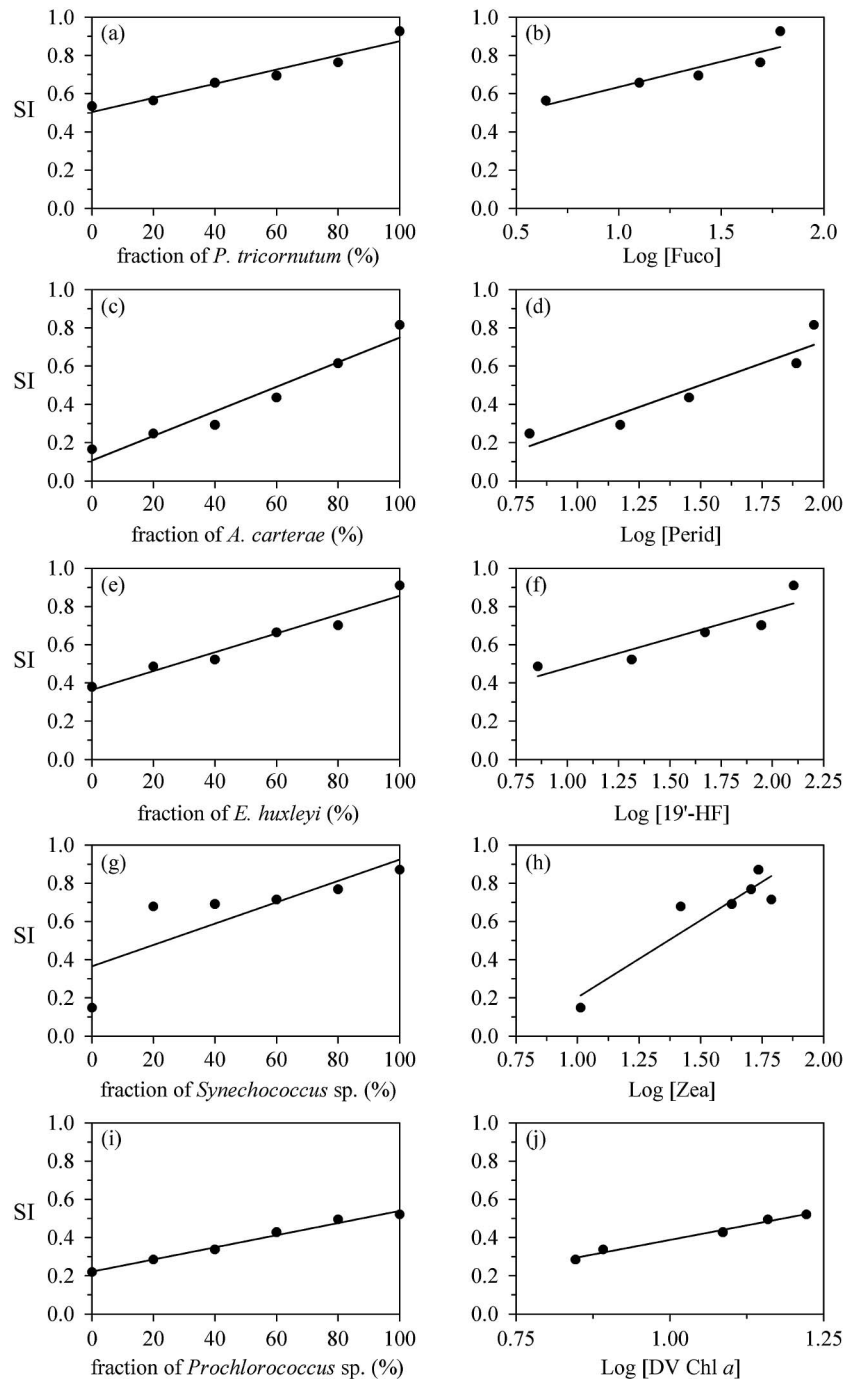


Fig. 6. Relationships between SI values, computed from the comparison between the fourth-derivative spectra of each assemblage and the spectrum of the species grown at $100 \mu\text{mol photons m}^{-2} \text{s}^{-1}$, and the relative fraction to TChl *a* (left column) or the logarithm of MP concentrations (right column) of a species within the mixed assemblages: (a) *P. tricorntutum*, (b) *A. carterae*, (c) *E. huxleyi*, (d) *Synechococcus* sp., (e) *Prochlorococcus* sp. Statistics of linear regressions are reported in Table 4.

Table 4. Parameters of Linear Regressions Displayed in Fig. 6: n = Number of Observations; B = Regression Slope; A = y -intercept; r^2 = Determination Coefficient^a

Equation	Species	Reference Spectrum	n	B ($\times 10^2$)	A	r^2	SI range
SI = $B * \%(\text{species}) + A$	<i>P. tricornutum</i>	ML	6	0.4	0.50	0.94 ^c	0.53–0.92
	<i>A. carterae</i>	ML	6	0.6	0.11	0.95 ^c	0.16–0.81
	<i>E. huxleyi</i>	ML	6	0.5	0.36	0.95 ^c	0.38–0.91
	<i>Synechococcus</i> sp.	ML	6	0.6	0.37	0.68 ^b	0.15–0.87
	<i>Prochlorococcus</i> sp.	HL	6	0.3	0.22	0.98 ^c	0.22–0.52
Equation	Marker Pigment	Reference Spectrum	n	B	A	r^2	SI Range
SI = $B * \text{Log}[\text{MP}] + A$	Fuco	ML	5	0.27	0.37	0.84 ^b	0.56–0.92
	Perid	ML	5	0.46	-0.19	0.89 ^b	0.25–0.81
	19'-HF	ML	5	0.31	0.17	0.83 ^b	0.49–0.91
	Zea	ML	6	0.81	-0.60	0.86 ^c	0.15–0.87
	DV Chl <i>a</i>	HL	5	0.61	-0.22	0.98 ^c	0.28–0.52

^aStudent's t -test:^b $p < 0.05$;^c $p < 0.01$.

results clearly indicated that the spectral signature of a given species substantially influences the bulk absorption spectrum of the assemblage. More importantly, results evidenced that the contribution of each species to the assemblage structure could be quantified using its absorption properties, also when the relative abundances of all contributing species were similar (i.e., 20% of TChl *a*).

However, the analysis of the variation ranges of the SI values and regression parameters (Table 4) suggested that the overall capability of discriminating a phytoplankton species using the bulk absorption spectrum of the assemblage was more or less robust depending on the considered species. For a null fraction (0%) of a given species (Fig. 6 left column), the SI values appeared to be always different from zero and were even high in the case of *P. tricornutum* and *E. huxleyi* (0.53 and 0.38, respectively; Table 4). They were, however, low for *A. carterae* (0.16), *Synechococcus* sp. (0.15), and *Prochlorococcus* sp. (0.22). This suggested that all the various reference spectra we studied shared some level of similarity in terms of shape. In addition, the similarity between the reference spectrum and the spectrum measured for an assemblage of 100% of a given species never reached 1, although they were cultured under the same controlled growth conditions. This may be because it is impossible to reproduce exactly the same absorption spectrum of a given species and for given growth conditions twice, as a consequence of multiple biological responses that organisms may have with respect to the same environmental factors. The impact of methodological errors cannot, however, be excluded. SI values were close to 1 in the case of *P. tricornutum* and *E. huxleyi* (0.92 and 0.91, respectively; Table 4), slightly lower for *Synechococcus* sp. (0.87) and *A. carterae* (0.81), and surprisingly low in the case of *Prochlorococcus* sp. (0.52). In particular, the case of *Prochlorococcus* sp. could be related to a low signal-to-noise ratio in those parts of the spectrum where there is no absorbing pigment [e.g., 550–650 nm for *Prochlorococcus* sp.; Fig. 5(e)], which could possibly affect the sensitivity of the fourth derivative method [18]. A comparison among replicates of spectra for those assemblages with 100% of a given species further strengthened the possible occurrence of methodological errors, as SI values no higher than

0.98 ± 0.003 (*E. huxleyi*) were observed. All regression slopes of linear models computed both with the relative abundance to TChl *a* (Fig. 6 left column) and MP concentrations (Fig. 6 right column) were significant, but high up to 0.81 only in the case of the cyanobacterium *Synechococcus* sp. [Table 4; Figs. 6(g)–6(h)]. The lower regression slopes especially for *P. tricornutum*, *A. carterae*, and *E. huxleyi* (Table 4) may be a consequence of the co-occurrence of similar pigment compositions and shared spectral shapes. In these cases, the level of similarity can lower performances in properly quantifying the presence of these algal groups from the bulk absorption spectrum of the assemblage.

3. Discrimination of a Given Species from Assemblages Adapted to Different Light Regimes

In this section, we evaluate the effects of light-induced spectral changes in the absorption coefficients for the quantification of a given species in assemblages with mixed taxonomic structure. Similar to the analyses presented in Section 3.B.2, we calculated the SI by pairwise comparison between each absorption spectrum of a simulated mixed assemblage (Fig. 5) and the spectrum of each given species when acclimated to different light growth conditions from the mixed assemblage as a reference, thus LL and HL (ML for *Prochlorococcus* sp.) spectra coming from Experiment 1 (Fig. 1). References obtained by averaging absorption spectra measured under the three light conditions (AS spectra, Fig. 3) of each given species were also used. The resulting SI was then regressed against the log10 concentration of the corresponding marker pigment within the mixed assemblage (Fig. 7).

The analysis of the variation ranges of SI values and regression parameters (Fig. 7, Table 5) revealed that the contribution of a species was detected within the absorption spectrum of a mixed assemblage, even when the reference spectra representing different light growth conditions were used. However, different behaviors were observed among species and according to the reference used. In the cases of *P. tricornutum*, *A. carterae*, and *E. huxleyi*, all SI values were significantly linearly correlated ($r^2 > 0.79$; Table 5) to the logarithm of concentrations of Fuco, Perid, and 19'-HF, respectively. Nevertheless, SI values

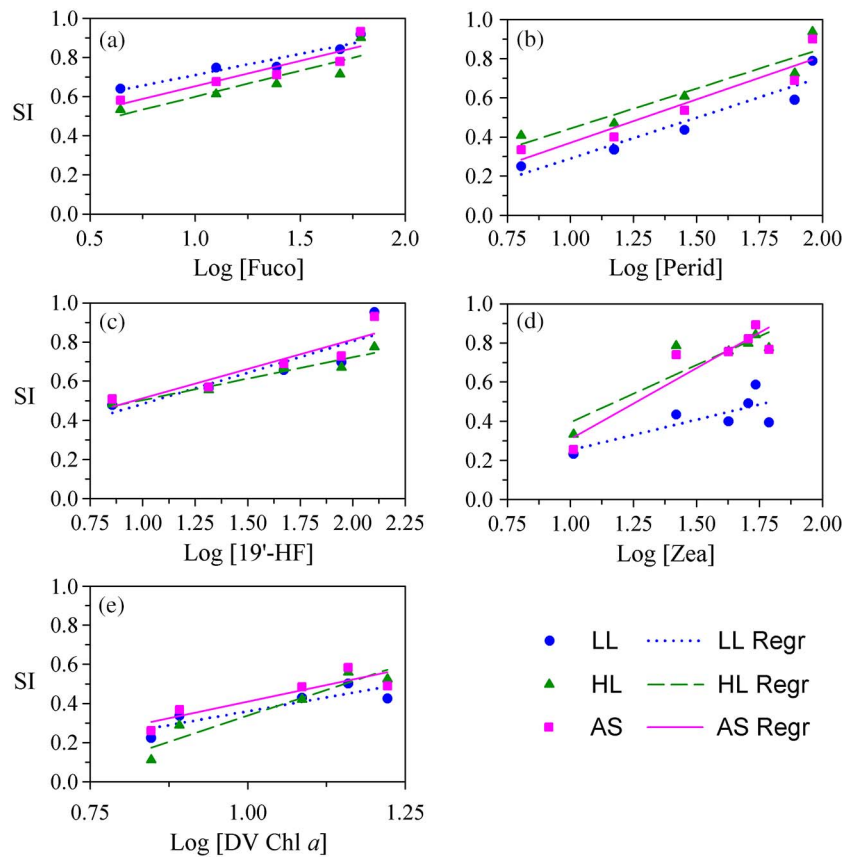


Fig. 7. As Fig. 6 (right column), for SI values obtained using reference spectra of species acclimated to LL, HL (ML for *Prochlorococcus* sp.) conditions and the AS spectra: (a) *P. tricornutum*, (b) *A. carterae*, (c) *E. huxleyi*, (d) *Synechococcus* sp., (e) *Prochlorococcus* sp. Statistics of linear regressions are reported in Table 5.

Table 5. Parameters of Linear Regressions Displayed in Fig. 7: *n* = Number of Observations; B = Regression Slope; A = *y*-intercept; *r*² = Determination Coefficient^a

Equation	Marker Pigment	Reference Spectrum	<i>n</i>	B	A	<i>r</i> ²	SI range
SI = B * Log[MP] + A	Fuco	LL	5	0.22	0.49	0.91 ^b	0.64–0.92
		HL	5	0.26	0.33	0.79 ^b	0.53–0.90
		AS	5	0.26	0.39	0.85 ^b	0.58–0.93
	Perid	LL	5	0.42	–0.13	0.90 ^b	0.25–0.79
		HL	5	0.41	0.03	0.88 ^b	0.41–0.94
		AS	5	0.44	–0.07	0.89 ^b	0.34–0.90
	19'-HF	LL	5	0.32	0.16	0.81 ^b	0.48–0.95
		HL	5	0.22	0.28	0.94 ^c	0.48–0.77
		AS	5	0.30	0.21	0.86 ^b	0.51–0.93
	Zea	LL	6	0.31	–0.06	0.60 ^{ns}	0.23–0.59
		HL	6	0.59	–0.19	0.82 ^b	0.33–0.84
		AS	6	0.72	–0.41	0.86 ^c	0.26–0.89
	DV Chl <i>a</i>	LL	5	0.57	–0.21	0.77 ^{ns}	0.22–0.50
		ML	5	1.06	–0.72	0.90 ^b	0.11–0.56
		AS	5	0.68	–0.27	0.80 ^b	0.26–0.58

^aStudent's *t*-test:

^b*p* < 0.05, ^{ns} not significant;

^c*p* < 0.01.

in *P. tricornutum* [Fig. 7(a)] were generally higher when the spectrum measured under the LL conditions was used as a reference instead of the HL or AS spectra (Table 5). The exact opposite situation occurred in *A. carterae*, for which the SI

values were maximum when the HL spectrum was used as the reference [Fig. 7(b), Table 5]. In the case of the two cyanobacteria *Synechococcus* sp. and *Prochlorococcus* sp., no significant relationships were found between SI and MPs when

absorption spectra of mixed assemblages were compared with the reference spectrum of the low irradiance condition [Table 5; Figs. 7(d)–7(e)]. This was probably a consequence of the high intraspecific spectral variability observed for these two species at the given experimental conditions.

The results of this experiment have implications in the context of operational application of algorithms used for the optical discrimination of phytoplankton groups. Frequently, in order to discriminate phytoplankton groups from spectra of assemblages with unknown taxonomic structure, absorption spectra of cultured or monospecific algal communities are used as a reference [17,23–25,75]. Evidently, this is made by assuming that similar growth conditions, and thus a similar level of photoacclimation, exist between the reference and the studied absorption spectrum. This can be a source of uncertainty affecting the performances of the retrievals. The next step was, therefore, to attempt to predict the concentration of the five marker pigments (and assess the errors) by applying the linear models shown in Table 5 to a range of SI values. The SI ranges, falling within the ranges observed from linear models (Table 5) and including SI values corresponding to increments of 0.05, were 0.65–0.90 for *P. tricornutum*, 0.45–0.75 for *A. carterae*, 0.55–0.75 for *E. huxleyi*, 0.40–0.80 for *Synechococcus* sp., and 0.30–0.50 for *Prochlorococcus* sp. Then we evaluated the predictive skills of the models by comparing the predicted MPs to the measured MPs in the different cultures. Because the five species used to obtain mixed algal assemblages were cultured at a light intensity of $100 \mu\text{mol photons m}^{-2} \text{s}^{-1}$, the MPs concentration obtained from linear models in Table 4 (i.e., comparison with ML-acclimated reference spectrum) were used as the measured MPs concentrations. RMSE% values (Eq. 2) were calculated for each statistically significant relationship of Table 5. RMSE% values varied from about 2% to 21% (Fig. 8). The HL-regression model generally produced RMSE% values higher than those resulting from the LL- and AS-regression models, except for *P. tricornutum*. MPs concentrations predicted from

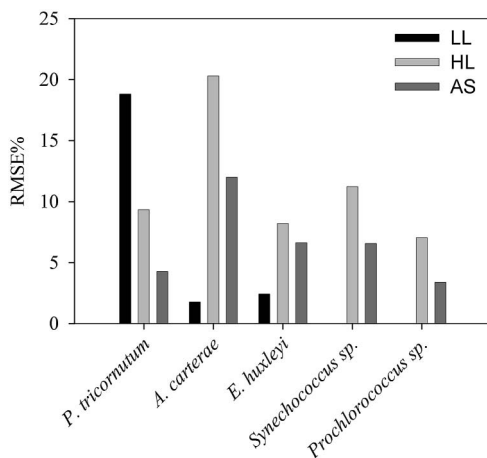


Fig. 8. RMSE% computed between the logarithm of MP concentrations estimated by LL, HL (ML for *Prochlorococcus* sp.), and AS regressions (Fig. 7) and those obtained from regressions in Fig. 6. MP concentrations were retrieved for a range of SI values representative of each species (see text). RMSE% values were calculated only for statistically significant regressions of Fig. 7 (see also Table 5).

AS-regression models were generally the lowest and ranged from 3% to 12% (Fig. 8). These results evidenced that the error in quantifying the abundance of different marker pigments representative of different taxonomic groups was generally low and slightly affected by changes in light growth conditions. In particular, these investigations showed that the average spectrum of three light conditions (AS spectrum) could actually reduce the error in quantifying the abundance of a given species within assemblages characterized by a mixed taxonomic composition.

4. CONCLUSIONS

Following the recommendations of the international community of phytoplankton functional type algorithm developers [12,43,44], two experiments on marine algal cultures representing different taxonomic groups were dedicated to investigate the extent to which the plasticity and/or similarity of spectral light absorption coefficients may affect the accuracy in optically detecting phytoplankton taxonomic composition. In particular, the datasets of pigments and light absorption spectra provided by the two presented experiments were exploited to specifically assess (1) what is the effect of light-driven spectral modifications in the accuracy of phytoplankton taxonomic composition retrievals by light absorption coefficients, and (2) how many phytoplankton groups can be discriminated from the bulk spectral light absorption properties of marine algal communities characterized by mixed taxonomic composition. The presented experiments were not intended for any algorithm development and/or validation.

Results of the two experiments showed encouraging directions to follow for improving current spectral absorption-based algorithms and/or exploring new approaches for the retrieval of multiple phytoplankton groups. In particular,

- The spectral signature of a given species substantially influences the bulk phytoplankton light absorption spectrum of the assemblage. Spectral signatures of five taxonomically different groups can be extracted and used for quantifying their relative contributions in terms of TChl *a* and marker pigment concentrations.
- Intraspecific plasticity of phytoplankton light absorption spectra due to changes in light conditions does not significantly affect optical classification and discrimination of five phytoplankton groups from assemblages with mixed taxonomic composition (RMSE% < 21%).
- The use of a reference spectrum coming from the average of various light regimes actually reduces the error in quantifying the abundance of a given species from bulk light absorption properties of mixed assemblages (RMSE% < 12%).
- The cyanobacteria, *Synechococcus* sp. and *Prochlorococcus* sp., can be discriminated as two separated groups within the same assemblage.

The analysis of the experiments also highlighted some limitations that might be taken in account when new algorithm development is planned and/or retrieval accuracy of the current approaches has to be evaluated. In particular,

- All light absorption spectra of the examined algal groups share some level of similarity in term of shape, which limits the accuracy of retrievals.

- The high spectral similarity observed between diatoms and dinoflagellates further reduces their discrimination capability when co-occurring within the same assemblage.

- Contributions <20% of a given group to TChl *a* within a mixed assemblage are hard to detect.

- Detection of the full dominance (i.e., 100%) of a given group using phytoplankton light absorption spectra is also affected by errors, which vary according to the group.

The analyses here presented are only the first step to understand the limits and to untangle the effects of growth light (photoacclimation/adaptation) in the detection of phytoplankton groups from bulk light absorption properties of assemblages with mixed taxonomic composition such those characterizing most oceanic environments. We acknowledge that there are some limitations to working with cultures and differences from natural populations (in terms of proportions among groups, total chlorophyll concentration of assemblages, and nutrient and light availability), but cultures represent the best way to individually assess the role of environmental factors acting in natural systems and the detection limits for a given algal group. A comparison of pigment distribution and bio-optical properties between simulated and natural algal assemblages suggested, however, that considerations resulting from these experiments could be extended also to open ocean waters and thus be relevant for improving methods of detection of phytoplankton from *in situ* and remote sensing platforms and for ecological and biogeochemical studies (e.g., primary production modeling [88]). It appears clear, however, that other aspects should be studied in depth in order to better simulate environmental conditions such as the analysis of the synergic effects of nutrient depletion and light limitation in modifying the spectral absorption coefficients and/or adding complexity to simulated taxonomic structures in terms of number of species and taxa. It is also envisaged to perform such experiments and analyses for spectral light backscattering coefficients in order to provide dedicated phytoplankton functional type algorithms [12,13] with similar information and to complement and/or enhance light absorption discrimination capabilities. Finally, since a hyperspectral resolution of ocean color sensors is planned for scheduled satellite missions [89], further efforts should be directed also to the investigation of the minimal spectral resolution required for achieving a comprehensive taxonomic knowledge of the phytoplankton community structure, in addition to specific groups [90], and at the same time make use of the technological and measurement maturity of hyperspectral sensors.

Funding. Università degli Studi di Firenze (Fondi di Ateneo 2008, 2009, 2010).

Acknowledgment. We acknowledge the Roscoff Culture Collection (<http://roscoff-culture-collection.org/>, France) for providing starting cultures of *Prochlorococcus* sp. (RCC 151), *Synechococcus* sp. (RCC 322), and *Emiliania huxleyi* (RCC 904). We warmly thank Marina Montresor of the Stazione Zoologica Anton Dohrn (Naples, Italy), who provided the algal culture of *Phaeodactylum tricorutum*, and the following colleagues of the Ecology and Plant Physiology Laboratory of the University of Florence (Italy): Chiara Melillo and

Mannuccio Mannucci for HPLC analysis; Giovanna Mori, Fabiola Fani, Francesca Polonelli, and Sara Masetti for helping during the execution of experiments. Robert Brewin (Plymouth Marine Laboratory, United Kingdom) is acknowledged for his useful comments and discussion on results. Data presented in this paper are available for distribution upon request (email to E. Organelli).

REFERENCES

1. C. S. Le Quéré, S. P. Harrison, I. C. Prentice, E. T. Buitenhuis, O. Aumont, L. Bopp, H. Claustre, L. Cotrim da Cunha, R. Geider, X. Giraud, C. Klaas, K. E. Kohfeld, L. Legendre, M. Manizza, T. Platt, R. B. Rivkin, S. Sathyendranath, J. Uitz, A. J. Watson, and D. Wolf-Gladrow, "Ecosystem dynamics based on plankton functional types for global ocean biogeochemistry models," *Glob. Change Biol.* **11**, 2016–2040 (2005).
2. J. Uitz, H. Claustre, B. Gentili, and D. Stramski, "Phytoplankton class-specific primary production in the world's oceans: seasonal and inter-annual variability from satellite observations," *Glob. Biogeochem. Cycles* **24**, GB3016 (2010).
3. G. Sarthou, K. R. Timmermans, S. Blain, and P. Tréguer, "Growth physiology and fate of diatoms in the ocean: a review," *J. Sea Res.* **53**, 25–42 (2005).
4. W. M. Balch, P. M. Holligan, S. G. Ackleson, and K. J. Voss, "Biological and optical properties of mesoscale coccolithophore blooms in the Gulf of Maine," *Limnol. Oceanogr.* **36**, 629–643 (1991).
5. W. Sunda, D. J. Kieber, R. P. Kiene, and S. Huntsman, "An antioxidant function for DMSP and DMS in marine algae," *Nature* **418**, 317–320 (2002).
6. S. Becagli, L. Lazzara, F. Fani, C. Marchese, R. Traversi, M. Severi, A. di Sarra, D. Sferlazzo, S. Piacentino, C. Bommarito, U. Dayan, and R. Udisti, "Relationship between methanesulphonate (MS) in atmospheric particulate and remotely sensed phytoplankton activity in oligo-mesotrophic central Mediterranean Sea," *Atmos. Environ.* **79**, 681–688 (2013).
7. S. Becagli, L. Lazzara, C. Marchese, U. Dayan, S. E. Ascanius, M. Cacciani, L. Caiazzo, C. Di Biagio, T. Di Iorio, A. di Sarra, P. Eriksen, F. Fani, F. Giardi, D. Meloni, G. Muscari, G. Pace, M. Severi, R. Traversi, and R. Udisti, "Relationships linking primary production, sea ice melting, and biogenic aerosol in the Arctic," *Atmos. Environ.* **136**, 1–15 (2016).
8. C. S. Reynolds, *The Ecology of Phytoplankton* (Cambridge University, 2006).
9. J. J. Cullen, A. M. Ciotti, R. F. Davis, and M. R. Lewis, "Optical detection and assessment of algal blooms," *Limnol. Oceanogr.* **42**, 1223–1239 (1997).
10. O. Schofield, J. Grzyski, W. P. Bisset, G. J. Kirkpatrick, D. F. Millie, M. Moline, and C. S. Roesler, "Optical monitoring and forecasting systems for harmful algal blooms: possibility or pipe dream?" *J. Phycol.* **35**, 1477–1496 (1999).
11. T. Platt, S. Sathyendranath, and V. Stuart, "Why study biological oceanography?" *Aquabio* **28**, 542–557 (2006).
12. IOCCG, "Phytoplankton functional types from space," Reports of the International Ocean-Colour Coordinating Groups no. 15 (IOCCG, 2014).
13. C. B. Mouw, N. J. Hardman-Mountford, S. Alvain, A. Bracher, R. J. W. Brewin, A. Bricaud, A. M. Ciotti, E. Devred, A. Fujiwara, T. Hirata, T. Hirawake, T. S. Kostadinov, S. Roy, and J. Uitz, "A consumer's guide to satellite remote sensing of multiple phytoplankton groups in the global ocean," *Front. Mar. Sci.* **4**, 41 (2017).
14. J. R. Moisan, T. A. Moisan, and M. A. Linkswiler, "An inverse modeling approach to estimating phytoplankton pigment concentrations from phytoplankton absorption spectra," *J. Geophys. Res.* **116**, C09018 (2011).
15. E. Torrecilla, D. Stramski, R. A. Reynolds, E. Millan-Nunez, and J. Piera, "Cluster analysis of hyperspectral optical data for discriminating phytoplankton pigment assemblages in the open ocean," *Remote Sens. Environ.* **115**, 2578–2593 (2011).

16. A. Chase, E. Boss, R. Zaneveld, A. Bricaud, H. Claustre, J. Ras, G. Dall'Olmo, and T. Westberry, "Decomposition of in situ particulate absorption spectra," *Methods Oceanogr.* **7**, 110–124 (2013).
17. A. M. Ciotti, M. R. Lewis, and J. J. Cullen, "Assessment of the relationships between dominant cell size in natural phytoplankton communities and the spectral shape of the absorption coefficient," *Limnol. Oceanogr.* **47**, 404–417 (2002).
18. E. Organelli, A. Bricaud, D. Antoine, and J. Uitz, "Multivariate approach for the retrieval of phytoplankton size structure from measured light absorption spectra in the Mediterranean Sea (BOUSSOLE site)," *Appl. Opt.* **52**, 2257–2273 (2013).
19. J. Uitz, D. Stramski, R. A. Reynolds, and J. Dubranna, "Assessing phytoplankton community composition from hyperspectral measurements of phytoplankton absorption coefficient and remote-sensing reflectance in open-ocean environments," *Remote Sens. Environ.* **171**, 58–74 (2015).
20. S. Wang, J. Ishizaka, T. Hirawake, Y. Watanabe, Y. Zhu, M. Hayashi, and S. Yoo, "Remote estimation of phytoplankton size fractions using the spectral shape of light absorption," *Opt. Express* **23**, 10301–10318 (2015).
21. D. F. Millie, O. M. Schofield, G. J. Kirkpatrick, G. Johnsen, P. A. Tester, and B. T. Vinyard, "Detection of harmful algal blooms using photopigments and absorption signatures: a case study of the Florida red tide dinoflagellate, *Gymnodinium breve*," *Limnol. Oceanogr.* **42**, 1240–1251 (1997).
22. G. J. Kirkpatrick, D. F. Millie, M. A. Moline, and O. Schofield, "Optical discrimination of a phytoplankton species in natural mixed populations," *Limnol. Oceanogr.* **45**, 467–471 (2000).
23. P. A. Stæhr and J. J. Cullen, "Detection of *Karenia mikimotoi* by spectral absorption signatures," *J. Plankton Res.* **25**, 1237–1249 (2003).
24. S. E. Craig, S. E. Lohrenz, Z. Lee, K. L. Mahoney, G. J. Kirkpatrick, O. M. Schofield, and R. G. Steward, "Use of hyperspectral remote sensing reflectance for detection and assessment of the harmful alga, *Karenia brevis*," *Appl. Opt.* **45**, 5414–5425 (2006).
25. B. Lubac, H. Loisel, N. Guiselin, R. Astoreca, L. F. Artigas, and X. Mériaux, "Hyperspectral and multispectral ocean color inversions to detect *Phaeocystis globosa* blooms in coastal waters," *J. Geophys. Res.* **113**, C06026 (2008).
26. T. Isada, T. Hirawake, T. Kobayashi, Y. Nosaka, M. Natsuike, I. Imai, K. Suzuki, and S. Saitoh, "Hyperspectral optical discrimination of phytoplankton community structure in Funika Bay and its implications for ocean color remote sensing of diatoms," *Remote Sens. Environ.* **159**, 134–151 (2015).
27. R. J. W. Brewin, N. J. Hardman-Mountford, S. J. Lavender, D. E. Raitsos, T. Hirata, J. Uitz, E. Devred, A. Bricaud, A. Ciotti, and B. Gentili, "An intercomparison of bio-optical techniques for detecting dominant phytoplankton size class from satellite remote sensing," *Remote Sens. Environ.* **115**, 325–339 (2011).
28. A. Morel and A. Bricaud, "Theoretical results concerning light absorption in a discrete medium, and application to specific absorption of phytoplankton," *Deep-Sea Res.* **28**, 1375–1393 (1981).
29. S. Sathyendranath, L. Lazzara, and L. Prieur, "Variations in the spectral values of specific absorption of phytoplankton," *Limnol. Oceanogr.* **32**, 403–415 (1987).
30. A. Bricaud, H. Claustre, J. Ras, and K. Oubelkheir, "Natural variability of phytoplanktonic absorption in oceanic waters: influence of the size structure of algal populations," *J. Geophys. Res.* **109**, C11010 (2004).
31. R. Bidigare, M. E. Ondrusak, J. H. Morrow, and D. A. Kiefer, "In vivo absorption properties of algal pigments," *Proc. SPIE* **1302**, 290–302 (1990).
32. N. Hoepffner and S. Sathyendranath, "Effect of pigment composition on absorption properties of phytoplankton," *Mar. Ecol. Prog. Ser.* **73**, 11–23 (1991).
33. S. W. Jeffrey, R. F. C. Mantoura, and T. Bjørnland, "Data for the identification of 47 key phytoplankton pigments," in *Phytoplankton Pigments in Oceanography*, S. W. Jeffrey, R. F. C. Mantoura, and S. W. Wright, eds. (UNESCO, 1997), pp. 449–559.
34. A. Morel, L. Lazzara, and J. Gostan, "Growth rate and quantum yield time response for a diatom to changing irradiances (energy and color)," *Limnol. Oceanogr.* **32**, 1066–1084 (1987).
35. H. M. Sosik and B. G. Mitchell, "Effects of temperature on growth, light absorption, and quantum yield in *Dunaliella tertiolecta* (Chlorophyceae)," *J. Phycol.* **30**, 833–840 (1994).
36. H. M. Sosik and B. G. Mitchell, "Light absorption by phytoplankton, photosynthetic pigments and detritus in the California current system," *Deep-Sea Res.* **42**, 1717–1748 (1995).
37. A. Bricaud, K. Allali, A. Morel, D. Marie, M. J. W. Veldhuis, F. Partensky, and D. Vaultot, "Divinyl chlorophyll *a*-specific absorption coefficients and absorption efficiency factors for *Prochlorococcus marinus*: kinetics of photoacclimation," *Mar. Ecol. Prog. Ser.* **188**, 21–32 (1999).
38. T. A. Moisan and B. G. Mitchell, "Photophysiological acclimation of *Phaeocystis antarctica* Karsten under light limitation," *Limnol. Oceanogr.* **44**, 247–258 (1999).
39. A. Sciandra, L. Lazzara, H. Claustre, and M. Babin, "Responses of growth rate, pigment composition and optical properties of *Cryptomonas* sp. to light and nitrogen stresses," *Mar. Ecol. Prog. Ser.* **201**, 107–120 (2000).
40. V. A. Lutz, S. Sathyendranath, E. J. H. Head, and W. K. W. Li, "Changes in the *in vivo* absorption and fluorescence excitation spectra with growth irradiance in three species of phytoplankton," *J. Plankton Res.* **23**, 555–569 (2001).
41. P. A. Stæhr, P. Henriksen, and S. Markager, "Photoacclimation of four marine phytoplankton species to irradiance and nutrient availability," *Mar. Ecol. Prog. Ser.* **238**, 47–59 (2002).
42. M. Laviale and J. Neveux, "Relationships between pigment ratios and growth irradiance in 11 marine phytoplankton species," *Mar. Ecol. Prog. Ser.* **425**, 63–77 (2011).
43. A. Bracher, N. Hardman-Mountford, T. Hirata, S. Bernard, E. Boss, R. Brewin, A. Bricaud, V. Brotas, A. Chase, A. M. Ciotti, J. K. Choi, L. Clementson, E. Devred, P. Di Giacomo, C. Dupouy, T. Hirawake, W. Kim, T. Kostadinov, E. Kwiatkowska, S. Lavender, T. Moisan, C. Mouw, S. Son, H. Sosik, J. Uitz, J. Werdell, and G. Zheng, "Phytoplankton composition from space: towards a validation strategy for satellite algorithms," NASA/TM-2015-217528 (2015).
44. A. Bracher, H. A. Bouman, R. J. W. Brewin, A. Bricaud, V. Brotas, A. M. Ciotti, L. Clementson, E. Devred, A. Di Cicco, S. Dutkiewicz, N. Hardman-Mountford, A. E. Hickman, M. Hieronymi, T. Hirata, S. N. Loza, C. B. Mouw, E. Organelli, D. E. Raitsos, J. Uitz, M. Vogt, and A. Wolanin, "Obtaining phytoplankton diversity from ocean color: a scientific roadmap for future development," *Front. Mar. Sci.* **4**, 55 (2017).
45. S. W. Jeffrey and M. Vesk, "Introduction to marine phytoplankton and their pigment signatures," in *Phytoplankton Pigments in Oceanography*, S. W. Jeffrey, R. F. C. Mantoura, and S. W. Wright, eds. (UNESCO, 1997), pp. 37–84.
46. M. Latasa, R. Scharek, F. Le Gall, and L. Guillou, "Pigment suites and taxonomic groups in prasinophyceae," *J. Phycol.* **40**, 1149–1155 (2004).
47. K. A. Steidinger and K. Tangen, "Dinoflagellates," in *Identifying Marine Phytoplankton*, C. R. Tomas, ed. (Academic, 1997), pp. 387–584.
48. R. W. Butcher, "An introductory account of the smaller algae of British coastal waters. Part IV. Cryptophyceae," *Fish. Invest.* **4**, 1–54 (1967).
49. J. Thronsdon, "The planktonic marine flagellates," in *Identifying Marine Phytoplankton*, C. R. Tomas, ed. (Academic, 1997), pp. 591–729.
50. R. R. L. Guillard and J. H. Ryther, "Studies of marine planktonic diatoms. I. *Cyclotella nana* Hustedt and *Detonula confervacea* (Cleve) Gran," *Can. J. Microbiol.* **8**, 229–239 (1962).
51. R. R. L. Guillard, "Culture of phytoplankton for feeding marine invertebrates," in *Culture of Marine Invertebrate Animals*, W. L. Smith and M. H. Chanley, eds. (Plenum, 1975), pp. 26–60.
52. M. D. Keller, R. C. Selvin, W. Claus, and R. R. L. Guillard, "Media for the culture of oceanic ultraphytoplankton," *J. Phycol.* **23**, 633–638 (1987).
53. R. Ripka, T. Coursin, W. Hess, C. Lichtlé, D. J. Scanlan, K. A. Palinska, I. Iteman, F. Partensky, J. Houmard, and M. Herdman, "*Prochlorococcus marinus* Chisholm et al. 1992 subsp. *pastoris* subsp. nov. strain PCC 9511, the first axenic chlorophyll *a*₂/*b*₂-containing cyanobacterium (*Oxyphotobacteria*)," *Int. J. Syst. Evol. Microbiol.* **50**, 1833–1847 (2000).

54. A. M. Wood, R. C. Everroad, and L. M. Wingard, "Measuring growth rates in microalgal cultures," in *Algal Culturing Techniques*, R. A. Andersen, ed. (Elsevier Academic, 2005), pp. 269–286.
55. J. Ras, H. Claustre, and J. Uitz, "Spatial variability of phytoplankton pigment distributions in the subtropical South Pacific Ocean: comparison between in situ and predicted data," *Biogeosciences* **5**, 353–369 (2008).
56. I. Siokou-Frangou, U. Christaki, M. G. Mazzocchi, M. Montesor, M. Ribera d'Alcalà, D. Vaqué, and A. Zingone, "Plankton in the open Mediterranean Sea: a review," *Biogeosciences* **7**, 1543–1586 (2010).
57. E. Organelli, C. Nuccio, C. Melillo, and L. Massi, "Relationships between phytoplankton light absorption, pigment composition and size structure in offshore areas of the Mediterranean Sea," *Adv. Oceanogr. Limnol.* **2**, 107–123 (2011).
58. S. Tassan and G. M. Ferrari, "An alternative approach to absorption measurements of aquatic particles retained on filters," *Limnol. Oceanogr.* **40**, 1358–1368 (1995).
59. LI-COR, "LI-1800UW underwater spectroradiometer instruction manual," Publication No 8405-0037 (1989).
60. M. Kishino, M. Takahashi, N. Okami, and S. Ichimura, "Estimation of the spectral absorption coefficients of phytoplankton in the sea," *Bull. Mar. Sci.* **37**, 634–642 (1985).
61. S. Tassan and G. M. Ferrari, "A sensitivity analysis of the 'transmittance-reflectance' method for measuring light absorption by aquatic particles," *J. Plankton Res.* **24**, 757–774 (2002).
62. A. Bricaud and D. Stramski, "Spectral absorption coefficients of living phytoplankton and nonalgal biogenous matter: a comparison between the Peru upwelling area and the Sargasso Sea," *Limnol. Oceanogr.* **35**, 562–582 (1990).
63. R. Röttgers and S. Gehnke, "Measurement of light absorption by aquatic particles: improvement of the quantitative filter technique by use of an integrating sphere approach," *Appl. Opt.* **51**, 1336–1351 (2012).
64. D. Stramski, R. A. Reynolds, S. Kaczmarek, J. Uitz, and G. Zheng, "Correction of pathlength amplification in the filter-pad technique for measurements of particulate absorption coefficient in the visible spectral region," *Appl. Opt.* **54**, 6763–6782 (2015).
65. F. Vidussi, H. Claustre, J. Bustillos-Guzmán, C. Cailliau, and J. C. Marty, "Determination of chlorophylls and carotenoids of marine phytoplankton: separation of chlorophyll *a* from divinyl-chlorophyll *a* and zeaxanthin from lutein," *J. Plankton Res.* **18**, 2377–2382 (1996).
66. R. G. Barlow, D. G. Cummings, and S. W. Gibb, "Improved resolution of mono- and divinyl chlorophylls *a* and *b* and zeaxanthin and lutein in phytoplankton extracts using reverse phase C-8 HPLC," *Mar. Ecol. Prog. Ser.* **161**, 303–307 (1997).
67. R. F. C. Mantoura and D. J. Repeta, "Calibration methods for HPLC," in *Phytoplankton Pigments in Oceanography*, S. W. Jeffrey, R. F. C. Mantoura, and S. W. Wright, eds. (UNESCO, 1997), pp. 407–428.
68. R. R. L. Guillard and M. S. Sieracki, "Counting cells in cultures with the light microscope," in *Algal Culturing Techniques*, R. A. Andersen, ed. (Elsevier Academic, 2005), pp. 239–252.
69. H. Hillebrand, C. D. Dürselen, D. Kirschtel, U. Pollinger, and T. Zohary, "Biovolume calculation for pelagic and benthic microalgae," *J. Phycol.* **35**, 403–424 (1999).
70. W. H. Kruskal and W. A. Wallis, "Use of ranks in one criterion variance analysis," *Am. Statist. Ass.* **47**, 583–621 (1952).
71. H. Levene, "Robust tests for equality of variances," in *Contributions to Probability and Statistics: Essays in Honor of Harold Hotelling*, I. Olkin and H. Hotelling, et al., eds. (Stanford University, 1960), pp. 278–292.
72. I. H. A. Sneath and R. R. Sokal, *Numerical Taxonomy* (Freeman WH and Company, 1973).
73. R. R. Sokal and F. J. Rohlf, "The comparison of dendrograms by objective methods," *Taxon* **11**, 33–40 (1962).
74. Ø. Hammer, D. A. T. Harper, and P. D. Ryan, "PAST: paleontological statistics software package for education and data analysis," *Palaeontologia Electronica* **4**, 1–9 (2001) [software].
75. A. M. Ciotti and A. Bricaud, "Retrievals of a size parameter for phytoplankton and spectral light absorption by colored detrital matter from water-leaving radiances at SeaWiFS channels in a continental shelf region off Brazil," *Limnol. Oceanogr.* **4**, 237–253 (2006).
76. R. R. Bidigare, J. H. Morrow, and D. A. Kiefer, "Derivative analysis of spectral absorption by photosynthetic pigments in the western Sargasso Sea," *J. Mar. Res.* **47**, 323–341 (1989).
77. L. Lazzara, A. Bricaud, and H. Claustre, "Spectral absorption and fluorescence excitation properties of phytoplanktonic populations at a mesotrophic and an oligotrophic site in the tropical North Atlantic (EUMELI program)," *Deep-Sea Res. I* **43**, 1215–1240 (1996).
78. H. A. Bouman, T. Platt, S. Sathyendranath, W. K. W. Li, V. Stuart, C. Fuentes-Yaco, H. Maass, E. P. W. Horne, O. Ulloa, V. Lutz, and M. Kyewalyanga, "Temperature as indicator of optical properties and community structure of marine phytoplankton: implications for remote sensing," *Mar. Ecol. Prog. Ser.* **258**, 19–30 (2003).
79. M. Davey, G. A. Tarran, M. M. Mills, C. Ridame, R. J. Geider, and J. LaRoche, "Nutrient limitation of picophytoplankton photosynthesis and growth in the tropical North Atlantic," *Limnol. Oceanogr.* **53**, 1722–1733 (2008).
80. L. Schlüter, F. Møhlenberg, H. Havskum, and S. Larsen, "The use of phytoplankton pigments for identifying and quantifying phytoplankton groups in coastal areas: testing the influence of light and nutrients on pigment/chlorophyll *a* ratios," *Mar. Ecol. Prog. Ser.* **192**, 49–63 (2000).
81. H. Xi, M. Hieronymi, R. Röttgers, H. Krasemann, and Z. Qiu, "Hyperspectral differentiation of phytoplankton taxonomic groups: a comparison between using remote sensing reflectance and absorption spectra," *Remote Sens.* **7**, 14781–14805 (2015).
82. A. Morel, "Consequences of a *Synechococcus* bloom upon the optical properties of oceanic (case 1) waters," *Limnol. Oceanogr.* **42**, 1746–1754 (1997).
83. J. Uitz, Y. Huot, F. Bruyant, M. Babin, and H. Claustre, "Relating phytoplankton photophysiological properties to community structure on large scales," *Limnol. Oceanogr.* **53**, 614–630 (2008).
84. A. Bricaud, M. Babin, A. Morel, and H. Claustre, "Variability in the chlorophyll-specific absorption coefficients of natural phytoplankton: analysis and parameterization," *J. Geophys. Res.* **100**, 13321–13332 (1995).
85. A. Bricaud, A. Morel, M. Babin, K. Allali, and H. Claustre, "Variations of light absorption by suspended particles with chlorophyll *a* concentration in oceanic (case 1) waters: analysis and implications for bio-optical models," *J. Geophys. Res.* **103**, 31033–31044 (1998).
86. E. Organelli, A. Bricaud, B. Gentili, D. Antoine, and V. Vellucci, "Retrieval of colored detrital matter (CDM) light absorption coefficients in the Mediterranean Sea using field and satellite ocean color radiometry: evaluation of bio-optical inversion models," *Remote Sens. Environ.* **186**, 297–310 (2016).
87. A. Bricaud, M. Babin, H. Claustre, J. Ras, and F. Tièche, "Light absorption properties and absorption budget of Southeast Pacific waters," *J. Geophys. Res.* **115**, C08009 (2010).
88. J. Uitz, D. Stramski, B. Gentili, F. D'Ortenzio, and H. Claustre, "Estimates of phytoplankton class-specific and total primary production in the Mediterranean Sea from satellite ocean color observations," *Glob. Biogeochem. Cycles* **26**, GB2024 (2012).
89. IOCCG, "Mission requirements for future ocean-colour sensors," Reports of the International Ocean-Colour Coordinating Groups no. 13 (IOCCG, 2012).
90. A. Wolanin, M. A. Soppa, and A. Bracher, "Investigation of spectral band requirements for improving retrievals of phytoplankton functional types," *Remote Sens.* **8**, 1–21 (2016).